مجلة جامعة دمشق للعلوم الأساسية
مجلد 41-عدد 1 (2025): 128- 143

Damascus University Journal for the Basic Sciences
Vol 41 No.1 (2025): 128 -143

إطار شبكة عصبونية تلافيفية للكشف عن مرض كوفيد-19 في صور التصوير المقطعي المحوسب

جورج أنور كراز [1]

[1]قسم الذكاء الصنعي ومعالجة اللغات الطبيعية، كلية الهندسة المعلوماتية – جامعة دمشق – سوريا
george.karraz@damascusuniversity.edu.sy

الملخص

كوفيد-19 هو فيروس RNA يسبب أمراضًا معدية تنتقل بين الحيوانات وتطورت بين البشر. هذه الفئة من مسببات الأمراض هي المسؤولة عن أمراض الجهاز التنفسي. ويشير فيروس كورونا إلى النتوءات التي تشبه التاج على السطح الخارجي للفيروس. في السنوات الأخيرة، حدث توسع في توظيف الأدوات المتقدمة في مجال معالجة الصور الرقمية وتحليلها(DIPA) لدعم من أجهزة التصوير الطبي للكشف الدقيق والمساعدة في تشخيص الكثير من الأمراض. من هذا المنطلق، نشأت الحاجة الملحة لتوظيف الذكاء الاصطناعي مكملاً لـ DIPA في الكشف عن الأمراض. في هذا البحث، نقترح نهجًا فعالاً لمعالجة صور الأشعة المقطعية للرئة بشكل تكيفي، ومن ثم اكتشاف احتمالية الإصابة بفيروس كورونا بناءً على مصنف يعتمد على الشبكة العصبونية التلافيفية CNN كأداة للتعلم العميق. لقد اخترنا مجموعة بيانات فيروس كورونا SARS-COV-2 المعروفة لمتلازمة الجهاز التنفسي الحادة الشديدة كمجموعة بيانات فعالة مقترحة في الأدبيات ذات الصلة لتدريب والتحقق من صحة نماذج الذكاء الاصطناعي التي يمكن أن يقترحها الباحثون فيما يتعلق بالكشف التلقائي عن وجود فيروس كورونا في صورة الأشعة المقطعية للرئة. من ناحية أخرى، تحتوي مجموعة بيانات SARS-COV-2 على حالات دراسة كافية من وجهة نظر إحصائية، مما يجعل أي نموذج ذكاء اصطناعي مطور قابلاً للتدريب والتحقق من صحته. استخدمنا 70% من إجمالي الصور المقدمة لـ SAR-COV-2 في مرحلة تدريب المصنف، و30% الأخرى في مرحلة الاختبار كبيانات غير مرئية لم يتم تضمينها أثناء مرحلة التدريب. أثبتت النتائج التي تم الحصول عليها نجاح أسلوبنا في مرحلتي التدريب والاختبار دون أي مشاكل مشهورة، مثل الإفراط في الملاءمة، أو الانحناء المبكر، أو الأداء غير المستقر. لذلك نؤكد جودة الأداء واستقرار نهجنا مع دقة محققة على البيانات غير المرئية تصل إلى 99٪ في اكتشاف وتمييز حالات الإصابة.

الكلمات المفتاحية: الشبكات العصبونية التلافيفية، كوفيد-19، SARS-COV-2، الشبكات العصبونية متعددة الطبقات، خوارزمية الانتشار العكسي المرن، مرشح غاوس، مرشح CLAHE، مرشح لابلاس.

تاريخ الإيداع: 2023/09/20
تاريخ الموافقة: 2023/11/06

ISSN (online): 2789-6366
http://journal.damascusuniversity.edu.sy/index.php/index/index

A Convolutional Neural Network Framework to Detect COVID-19 Disease in Computerized Tomography Images

George Anwar Karraz [1]

[1]Department of Artificial Intelligence and Natural Language Processing ,Faculty of Information Technology Engineering
Damascus University- Syria george.karraz@damascusuniversity.edu.sy

Abstract

COVID-19 is an RNA virus that causes infectious diseases that are transmitted between animals and have evolved among humans. This class of pathogens is responsible for respiratory diseases. Coronavirus refers to the crown-like protrusions on the outside surface of the virus. Commonly, coronavirus is an infection that causes breathing difficulties in humans. In recent years, there has been an expansion in employing symptom investigation techniques based on advanced tools in the field of digital image processing and analysis DIPA, which are essential for deeply examining disease symptoms, and lead to better results obtained from medical imaging devices for identifying and diagnosing a lot of diseases. From this standpoint, the urgent need to employ artificial intelligence as a supporter of DIPA in disease detection arose. In this research, we propose an efficient approach to manipulate the lung's CT-scan images adaptively, and then detect the probability of coronavirus infection based on a sophisticated classifier based on the convolutional neural network CNN as a deep learning tool. We chose the well-known severe acute respiratory syndrome coronavirus 2 SARS-COV-2 dataset as an efficient dataset proposed in the relevant literature to train and validate the artificial intelligence models that could proposed by researchers related to detecting automatically the presence of coronavirus in the lung's CT-scan image. On the other hand, the SARS-COV-2 dataset contains sufficient study cases from a statistical point of view, that makes any developed AI model able to be trained and validated. We used 70% of the total images presented in SAR-CoV-2 in the classifier's training phase, and the other 30% in its testing stage as unseen data that was not involved during the training phase. The obtained results proved the successful performance of our approach in both the training and testing phases without any famous encountered problems, such as over-fitting, early stooping, or unstable performance. So we confirm the performance quality and stability of our approach with achieved accuracy over unseen data of up to 99% in detecting and distinguishing the infection cases.

Received :2023/09/20
Accepted:2023/11/06

Keywords: Convolutional Neural Networks CNN, COVID-19, SARS-COV-2, Multilayer Neural Networks MLNN, Resilient Backpropagation Algorithm RBP, Gaussian Filter G-F, CLAHE Filter, Sharpening Filter S-F.

1. Introduction

The global community is currently facing a novel health crisis that threatens public health due to the rapid transmission of the COVID-19 virus (Coronavirus Disease). The emergence of COVID-19 in December 2019 at the Hunan seafood market in Wuhan, South China, and its subsequent global spread has led to the World Health Organization (WHO) declaring that the coronavirus is an international public health emergency. Both the number of infected individuals and the mortality rate are rising. Fever, dry cough, myalgia, dyspnea, and headache are the most typical symptoms of the novel Coronavirus. Nonetheless, in some cases, the absence of symptoms (asymptomatic) makes the disease a more significant hazard to public health (Islam et al.,2021, 30551–30572). COVID-19 has been demonstrated to be among the most dangerous ailments severely threatening human civilization (Herpest et al.,2021, 81-87). With the advancement of modern technology over the past few decades, ingenious tools and facilities have been developed to aid in disease diagnosis, prevention, and control. Specifically, imaging modalities such as CT and X-ray are among the most effective for COVID-19 diagnosis (Kovács et al., 2021, 2819–2824). COVID-19 disease is still developing rapidly and causes deaths in the elderly. Therefore, the aim of the research is early detection based on artificial intelligence which is the simulation of human intelligence processes by machines, primarily computer systems. Often AI works with machine learning ML which refers to an algorithm-based intelligent artificial system that is self-learning. ML can demonstrate increasing levels of innovation and intelligence without direct human intervention. The second innovation is in the discipline of deep learning DL. The application of machine learning techniques to the examination of massive data collections. The advancement of machine learning is guided by the principles of exactness and velocity (Bi, et al., 2019, 2222-2239). DL differentiates itself from conventional ML techniques by utilizing multiple layers that enhance abstraction and robust generalization. Utilizing neural networks requires extracting attributes to reduce the networks' computational burden. For neural networks to integrate features, it is necessary to reduce the overlapped attributes. Essential will be establishing a comprehensive network capable of communicating precise directives (Yousif, et al., 2020, 195–208). Therefore, Training's likelihood of success was minimal or nonexistent. Due to computing power and memory capacity advances, it is now feasible to train large networks effectively. In the same deep-learning network, both feature extraction and classification/generalization can be executed, yielding significant advantages (Piramuthu, 1999, 310–321). A DL model's precision depends on the accuracy of the training or validation dataset. In data science, model training involves applying the optimal weights and biases to a machine learning algorithm to minimize a loss function across the prediction range (Jiang et al.,2023,1-14), for this reason, it is better to involve and activate the pre-trained models in DL methodologies.

Deep learning based on convolutional neural networks has been presented in related scientific research, mainly to support algorithms for recognizing objects in digital images (Valueva et al., 2020, 232–243), within the framework of computer vision, which is considered one of the most important fields of artificial intelligence. During the last decade, many convolutional neural network structures have been presented to recognize objects in certain images, including but not limited to medical images. We mention the most important developed models:

• ResNet: is a computer vision deep learning model. Its CNN framework supports hundreds or thousands of convolutional layers, it has a limitations related to occupying a large space of memory Accompanied by slow implementation of the learning process, and the probability of vanishing the gradient of the training cost function that leads to early stopping of the learning algorithm without reaching the optimum solution and low rate of accuracy in the testing stage (Wu et al., 2023, 1-10).

• U-Net: Semantic U-Net segmentation. It resamples or reduces the input data through up-adding two convolutions and then maximum pooling algorithms by using a kernel with size 3x3 and 2x2 respectively, with a possibility to replicate the process depending on the studied problem (Zhang et al., 2023, 13), this technique has been succeeded on some applications, whereas gave a moderate performance in much of others.

• AlexNet: It loads an image and executes eight layers of convolution, then trains a neural network to classify magnetic resonance imaging MRI images to predict different brain disorders (Alsharabi et al., 2023, 1-20), taking into account the difference in the criteria of manipulating images took by CT-scan and MRI., because

when an abnormal image is presented, the CT-scan image has a higher ratio of interference between the disease and benign details than MRI image.

• Very Deep Convolutional Network (VDCNet) for large-scale image processing, it was proposed to increase the learning depth by using an architecture with convolution filter of very small kernel's size (3x3) (Simonyan et al., 2015, 1-14), and recently (Ijaz et al., 2023, 15750–15762) confirmed again how VDCNet depth affects accuracy in limited conditions.

2. Problem Description

Many challenges are facing the DL models presented in the medical field, the main one regards the interference of disease-marking features with other normal details present in medical images, which leads to the presence of a complex nonlinear mathematical problem is difficult to solve, thus the accuracy of the proposed model decreases in accurately detecting the desired object. Add to that the complexity in the structure of the proposed models and the excessive load on the structure during the process of training it on specific models, which requires a long time in learning and the exploitation of an excess amount of computer memory as a result of the great complexity of the computer operations included in the model and a high probability of problems occurring during the training phase that affect the model's stability. So the model wouldn't be trained optimally, and thus it does not reach the ideal solution, which leads to a decrease in its accuracy or obtaining moderate accuracy while testing it on unseen data during the testing phase. This issue negatively affects performance, especially in applications of a medical nature. As is the case with the topic of our research.

3. Motivation and Objectives

The primary motivation behind this research is to overcome a set of meaningful challenges and gaps that face related research to reach an accurate model to detect coronavirus presented in medical CT-scan images. So in this research, we suggest a model based on two tools that work together. The first one is related to image processing to reduce noise that can affect fine details in the image, such as Gaussian noise. On the other hand, this tool works to remove or reduce the intensity of some color values of the studied image elements in a way that ensures the clarity of the image, to indicate carefully the features associated with the presence of the disease at the expense of features associated with other non-pathological details present in the image. The other tool is an adaptive convolutional neural network with a simple structure at two convolution levels and employing the resilient backpropagation learning algorithm RBP, Due to the merit of RBP for solving non-linear problems with binary classification is compatible with the merits of our scientific problems presented in this research, which are represented by random and non-linear placement of the effect detected in the studied images as a result of infection with the coronavirus, then reach the primary goal is to classify the images in a binary form as healthy or non.

4. Literature Review

Many previous studies have been addressed by different researchers on detecting coronavirus in medical images. (Owida et al., 2022, 1-14) proposed a system that investigates how to identify COVID-19 using computational tomography (CT) scans by employing a DL technique derived from the enhancement of ResNet architecture, and they concluded by aiming for future work to improve the obtained results. (Aslan, 2022, 1447-1463) predicted COVID-19 accurately by using CT images, the developed model based on applying AlexNet. Firstly, mAlexNet architecture is built and classified, whereas secondly the time series analysis TSA was involved to optimize ANN to classify images by using 25 features. It's notable through this hetero model its unneeded architecture complexity is imposed from reaching the optimum solution in the training stage of the suggested ANN.

(Mehboob et al, 2022, 1-12) proposed a model to investigate the identification of COVID-19 using computed tomography (CT) imaging by employing a deep learning technique derived from enhancing ResNet architecture, with a limited dataset and moderate obtained results concluded in the model's testing phase.

(Xu et al., 2022, 2931–2949) suggested the sine-cosine algorithm side-channel analysis (SCA) to optimize the deep convolutional neural network DCNN structure for raw CT image status determination, three regular SCA-based enhancements increase accuracy and speed, IP-based encoding is suggested, an enfeebled layer generates a variable-length DCNN, the developed system was trained and tested by using SARS COV 2 datasets. The suggested model realized a moderate accuracy aiming to improve it as a future work.

(Shah et al., 2021, 1-22) suggested an image recognition tool can learn to identify and describe objects in images by analyzing a lot of examples and concluded that the ideal characteristic of artificial intelligence is the capacity to reason and take actions with the highest probability of attaining a specific objective, that is well-known in the artificial intelligence's literature. So this research didn't give any additional knowledge.
(Islam et al.,2021, 30551–30572) proposed a medical system that can detect infected people from non-infected people in coronavirus, DL algorithms are trained and tested on a limited dataset volume. So the authors didn't prove efficiently the generalizability of their suggested approach.

5. Suggested Approach

Based on the SARS-COV19-2 dataset we propose an intelligent system to detect accurately the infection in coronavirus among a set of CT-scan images of the lung region, on the other hand, we take into account the simplicity in architecture and training algorithm, and in other hand overcome a set of gaps and challenges encountered in previous related research. Our suggested system operates efficiently in two stages, the first one is the preprocessing stage and the second one is the classification stage. Figure. 1 shows the block diagram of the proposed system stages.

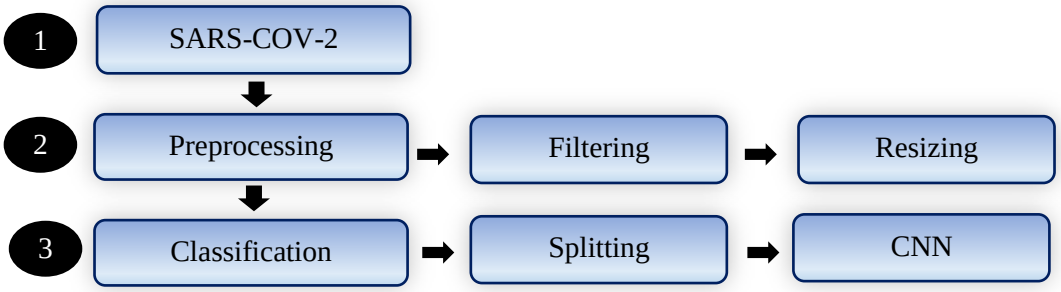

Figure1. A bock diagram of proposed system

5.1. Data Collection

In this research, we employ the SARS-COV-2 CT-scan dataset (Soares, et al., 2020). It consists of 2482 CT images from 120 patients, including 1252 CT images from 60 infected patients (32 males and 28 females) and. 1230 CT images of 60 non-infected patients (30 males and 30 females). The images in this dataset are digital photographs of printed CT assessments, and there is no standard for image size. Whereas, the smallest image in the dataset has dimensions of 104 by 153, while the largest image has dimensions of 484 by 416. Table 1 summarizes the SARS-COV 2 CT dataset. We denote the total number of images representing infected cases Cp and Cn for those representing non-infected cases. Image size represents the number of pixels in both image length and width. Figure 3-1 illustrates an example of an image in the SARS-COV 2 CT dataset.

Table 1. The SARS-C0V-2 CT dataset

Patients		Sex		Images
Type	No. Patients	M	F	
Infected	60	32	28	1252
Non-infected	60	30	30	1230
Total	120			2482

5.2. Preprocessing

In the preprocessing stage, we employ three sequence filters in the spatial domain of studied image, each of these filters has a small kernel of size (3x3) containing nine filter factors, and the output image of each selected filter

represents the convolution between the input image and the related filter's kernel. The first filter is Gaussian Filter G-F which is selected to smooth the studied images and remove the possibility of the Gaussian noise effect that may occur widely in medical images, On the other hand, G-F enhances smoothing the presence of noise that may affects the medical images by intensity values with high frequency level and leads to not revealing some important details from the studied image. In case of applying G-F with the absence of noise there isn't any changes will be taken place or any lose in information in studied image. The second filter is the CLAHE filter as it is well-known for enhancing the local contrast of the studied image according to the sparse distribution of the high-intensity value of infected regions, The CLAHE filter operates on small regions of images called tiles better than the entire image. The neighboring tiles are then combined using bilinear interpolation to remove the artificial boundaries, the operation of the CLAHE filter is applied on the image and in a way varies corresponding to adaptive histogram equalization AHE. The third filter is Sharpening Filter S-F to enhance the sharpness of the studied image, it operates by subtracting the blurred image from the original one, so in this case we smooth the obtained image from the CLAHE filter by the first G-F then we subtract the smoothed image from previous one of CLAHE filter. Finally, we resized all the filtered images in our dataset, so each filtered image was represented in size (216 * 216) pixels. Figure 2 illustrates schematically the preprocessing stages, whereas Figure 3 illustrates the performance of preprocessing stages on a studied Image from our selected dataset.

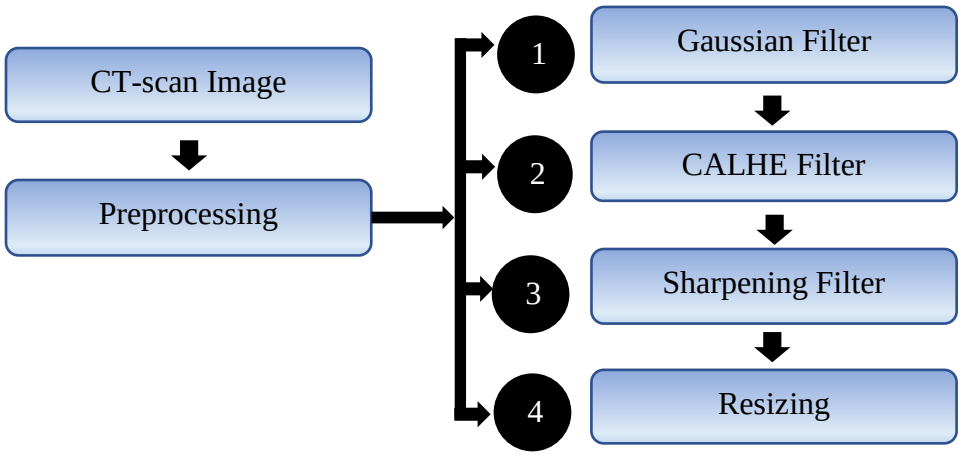

Figure 2. Schematic diagram of preprocessing stag

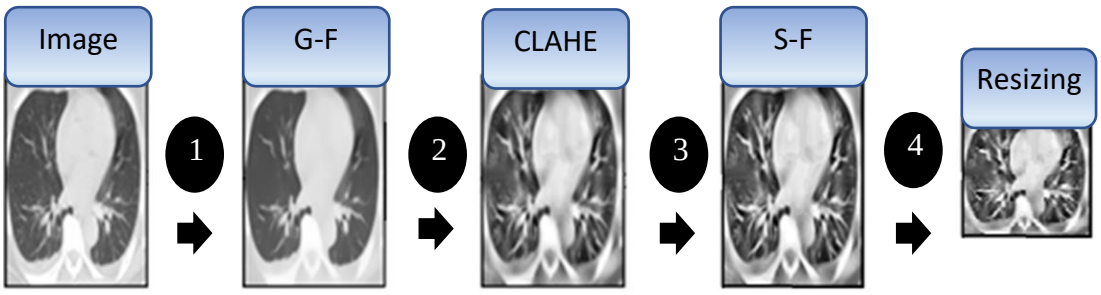

Figure 3. Performance of preprocessing stages on a studied Image

5.3. Classification

5.3.1. Architecture

We employ CNN to classify each studied image in a binary class representing infected or non-infected cases, as is well known CNN is a DL tool, and it is also a class of artificial neural networks basically applied to analyze the digital images. CNNs use a mathematical operation called convolution in place of the general matrix in at least one of their layers (Goodfellow et al., 2016, 326). CNN is specifically designed to process pixel data and is used in image recognition and processing. The main steps involved in applying a CNN are illustrated in Figure 4 below, the first step is the convolution by applying a Laplacian L-F edge detector on the studied image by using a kernel size (3 x 3), the used kernel is mentioned in Figure 4, the second step is to perform a max pooling process on each image segment of (3 x 3) pixels scanned by the L-F during the previous convolution step, through this step we create a new image by replacing the intensity values of each image segment with only one element that represent the max value of the intensity values presented in image segment, this step reduces the size of the image by one-ninth according to the total number of factors presented in the filter kernel. We repeat the first and the second steps sequentially three times, each time reducing the image size by one-ninth, so finally we obtain an image with size (8 x 8) pixels from the original one of size (216 x 216) pixels. The third step flattens the extracted image from the previous steps into a features vector of size (64 x 1) which represents the input of the fourth step, which performs a multilayer feedforward neural network MLNN, that could be trained and tested to classify its input (features vector) in a binary class infected or non which is encoded by 1 and 0 respectively, according to the target given from the description of each image in the selected database. We executed a lot of experiments to select the best MLNN architecture that guarantees the best performance and leads to reaching correctly the classification stage. The executed experiments concluded that in our case the best architecture is four layers: The input layer contains 64 neurons according to the size of the extracted features vector from the previous step, then two sequential hidden layers contain 32 and 16 neurons respectively, then the output with only one neuron to reveal the binary classification values: 1 and 0 according to infected and non-infected cases respectively. MLNN architecture is illustrated in Figure 4 below.

5.3.1. Learning Algorithm

MLFNN is trained in different regarded training algorithms RBP, Quasi-Newton QN, Levenberg Marquardt LM, and Bayesian BAY, The Training dataset forms 60% of all our selected dataset SARS COV 2 CT-Scan, so it contains 1490 images, the experiments proved, that the RBP algorithm realizes the best performance comparing with other selected algorithms. RBP is considered one of the best methods for solving nonlinear binary prediction; RBP has been proposed in the artificial intelligence literature to address the weaknesses of the classical backpropagation algorithm BP, and its drawbacks with long training times and to speed up the learning process RBP works by directly adapting the weights based on local gradient information at each learning iteration, thus modifying the weights and bias network. The mean squared error (MSE) values are reduced and accuracy is improved. The algorithm elaborates on each weight separately. If the sign of the partial derivation of the error changes compared to the sign of the previous iteration, the updated value of the correlated weights is multiplied by a factor of η-, where $0 < \eta - < 1$, and if the sign remains the same as in the last iteration, the updated value is multiplied by a factor of η +, where $\eta + > 1$. That is, each weight is modified by the updated value of the associated partial derivation in the opposite direction. η+ and η- are empirically chosen to be 1.2 and 0.5, respectively. The algorithm starts by giving the initial value of each weight *wii* and its updated value Δj (t). The updated values are then changed according to a learning rule based on the sign of the partial derivation of the associated error, and the weight values on which they depend are updated. The mathematical conditions described above are illustrated
in Equation 1 below.

$$\Delta_{ij}(t) =$$

$$\eta^{+}.\Delta_{ij}(t-1) \quad if \quad \frac{\partial E}{\partial w_{ij}}(t).\frac{\partial E}{\partial w_{ij}}(t-1) > 0$$

$$\eta^{-}.\Delta_{ij}(t-1) \quad if \quad \frac{\partial E}{\partial w_{ij}}(t).\frac{\partial E}{\partial w_{ij}}(t-1) < 0$$

$$\Delta_{ij}(t-1) else$$

Whenever Equation 2 reveals a case where the partial derivation associated with *wi*Ņ changes sign, it indicates that a large update value has occurred and the algorithm has exceeded the local minimum of the error, so the update value Δ(t) is decreased or increased by a factor η- based on positive or negative partial derivation, respectively.

$$\Delta w_{ij} =$$

$$-\Delta_{ij}(t) \text{ if } \frac{\partial E}{\partial W_{ij}} > 0$$

$$\Delta_{\mathrm{ij}}(\mathrm{t}) \quad \text{if} \quad \frac{\partial \mathrm{E}}{\partial \mathrm{W_{ij}}} < 0$$

Equation 3 shows that when the correlated partial error derivation is negative, the new updated weights are computed from the previous ones by adding the updated values. The converse is to subtract the updated values when the derivation of the correlated partial error is positive.

$$\mathrm{W_{ij}}(\mathrm{t}+1) = \mathrm{W_{ij}}(\mathrm{t}) + \Delta \mathrm{W_{ij}}(\mathrm{t}) \qquad (3)$$

Equation 4 shows an exceptional case where the derivation of the partial error changes, indicating that the local minima of the error were skipped because the previous update was too large. In this case, the algorithm undoes the previous weight update

$$\Delta \mathrm{w_{ij}}(\mathrm{t}) = -\mathrm{w_{ij}}(\mathrm{t}-1)$$

$$\text{If } \frac{\partial \mathrm{E}}{\partial \mathrm{w_{ij}}}(\mathrm{t}).\frac{\partial \mathrm{E}}{\partial \mathrm{w_{ij}}}(\mathrm{t}-1) < 0 \qquad (4)$$

The derivation of the partial error may change sign again in the next step, in which case the algorithm avoids a double update by setting Ewij (t-1) = 0 in the above update rule in Equation 4. Equation 5 describes the calculation of the partial derivation of the total error

$$\frac{\partial E}{\partial W_{ij}} = \frac{1}{2}\sum_{p=1}^{p}\frac{\partial E_p}{\partial W_{ij}} \qquad (5)$$

RBP reached a minimum training mean squared error is about 0.024 in 45 minutes of training time and 1058 of training iterations, whereas the other selected algorithms couldn't reach the RBP error over a long time of training, because the training curve of other selected algorithms reached a high error value and remained

stationary to the end of training iterations. Figure 5 illustrates the performance of RBP during its training phase. RBP proved its training stability by the stable value of mean squared error after reaching the local minima related to the best solution obtained during the training phase, which means that the approximation towards the local minima has been reached without any future crossover of the best solution in an infinite number of iteration, in other words, the instability of training process. On the other hand, the training phase was executed without any problems which led to bad classification such as the overfitting, vanishing of the gradient of mean squared error, early stooping, and reaching a suboptimal solution after a huge number of iterations with unreasonable training time. Table 2 below illustrates a clear comparison between the behavior and the performance of RBP and other selected algorithms during the training phase to solve our suggested problem in this research.

Table 2. Performance comparison of various learning algorithms during the training phase.

Learning Algorithm	Performance
L M	Local optimum of errors is not stable
BAY	Local optimum of errors is not stable
QN	Learning stops early with a suboptimal error
RBP	Optimal and stable performance

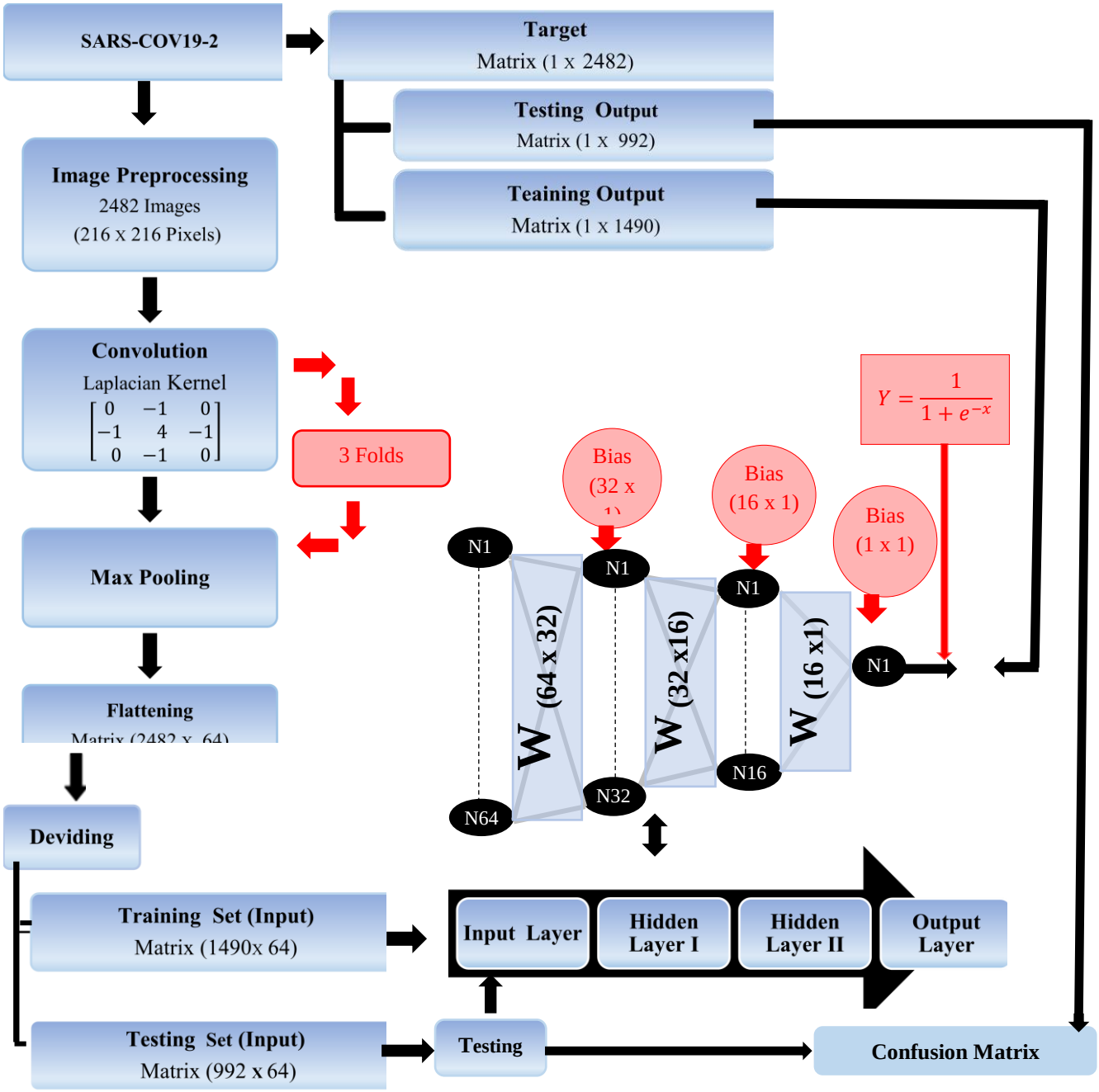

Figure 4. The structure of the classification stage

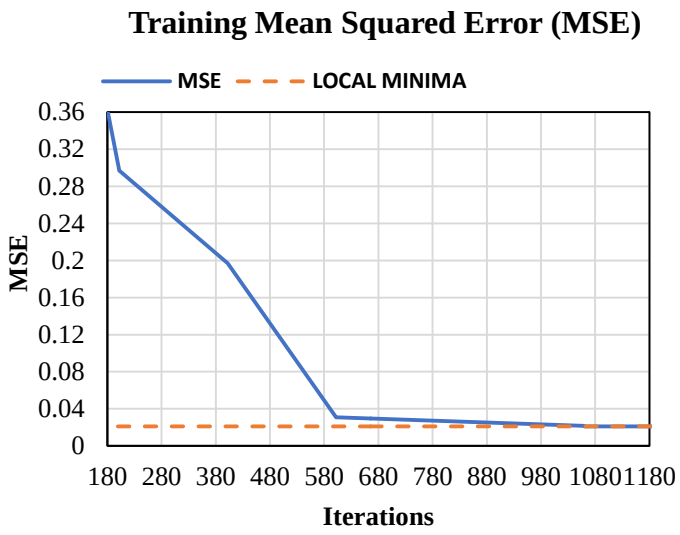

Figure 5. The performance of RBP during its training phase

5.3.2. Testing and Validation

The developed classifier is tested on a testing dataset that forms 40% of our selected dataset SARS-COV-2 CT-Scan) and contains 992 images, 500 infected (positive) and 492 non-infected(negative), to evaluate the results we calculated the values of the confusion matrix regarding the number of total real positive cases Cp, real negative Cn, the true predicted positive cases Tp, true predicted negative cases Tn, false positive predicted cases Fp, and false negative predicted cases Fn. Table 3. Illustrates the values of the confusion matrix.

Table 3. Confusion matrix.

Cp	Cn	Tp	Tn	Fp	Fn
500	492	495	489	3	5

According to the values presented in the confusion matrix, we used four statistical functions to calculate the sensitivity Se, specificity Sp, and accuracy Acc these functions represent the system's capacity to recognize correctly the positive cases, negative cases, and both respectively, where the error (Err) represents the probability of both false positive and negative cases, see Equations 6, 7, 8 and 9 illustrate how we calculate Se, Sp, Acc, and Err, respectively. Table 4 illustrates the results of the statistical evaluation process.

$$S_e = \frac{T_p}{C_P} \quad (6) \qquad S_p = \frac{T_n}{C_n} \quad (7) \qquad A_{CC} = \frac{T_{n+}T_P}{C_n + C_p} \quad (8) \qquad E_{rr} = 1 - A_{CC} \quad (9)$$

Table 4. The results of statistical evaluation process

S_e	S_p	A_{CC}	E_{rr}
0.99	**0.993**	**0.992**	**0.008**

One of the efficient statistical methods to evaluate our results is using the receiver operating characteristics curve (ROC) which represents the relationship between the probabilities of true detected positive cases (Se) and the probabilities of false positive detected cases (1- Sp), ROC reports an index about the model's capacity of recognizing the infected and non-infected cases (https://www.towardsdatascience.com/understanding-auc-roc-curve), and measures the separability degree of classification, the probabilities used in ROC curve is calculated according to hundred thresholds in the range [0 1]. we calculated according to every selected threshold the sensitivity and specificity of the classifier, the obtained results proved that the best threshold is 0.54, <0.54 for

the negative cases and >=0.54 for the positive cases, then we plotted the ROC curve as illustrated in Figure 6, we also calculated the area under ROC (AUC) as an important index to evaluate the classifier efficiency, the classifier which realizes AUC more than 0.9 is considered to have a perfect efficiency, the AUC is representing statistically the mean of sensitivities at the selected thresholds, AUC in our system is 0.95. Figure 7 illustrates a test validation comparison between the different well-known MLNN algorithms with RBP. Figure 8 reports two examples of classification stage for both infected and non-infected cases

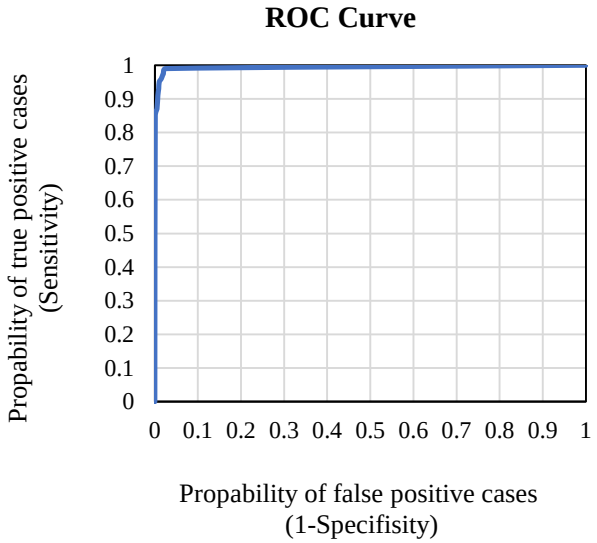

Figure 6. ROC curve

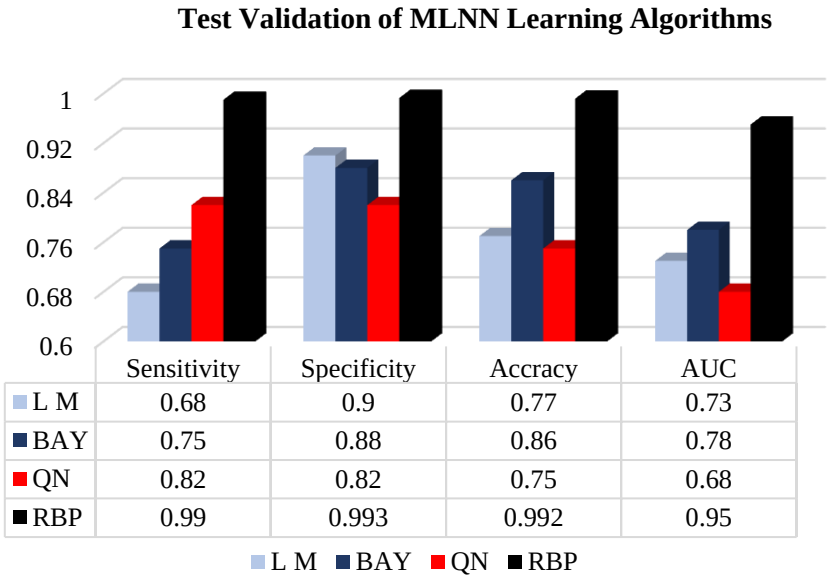

Figure 7. Test validation comparison between the different selected MLNN algorithms

(A)

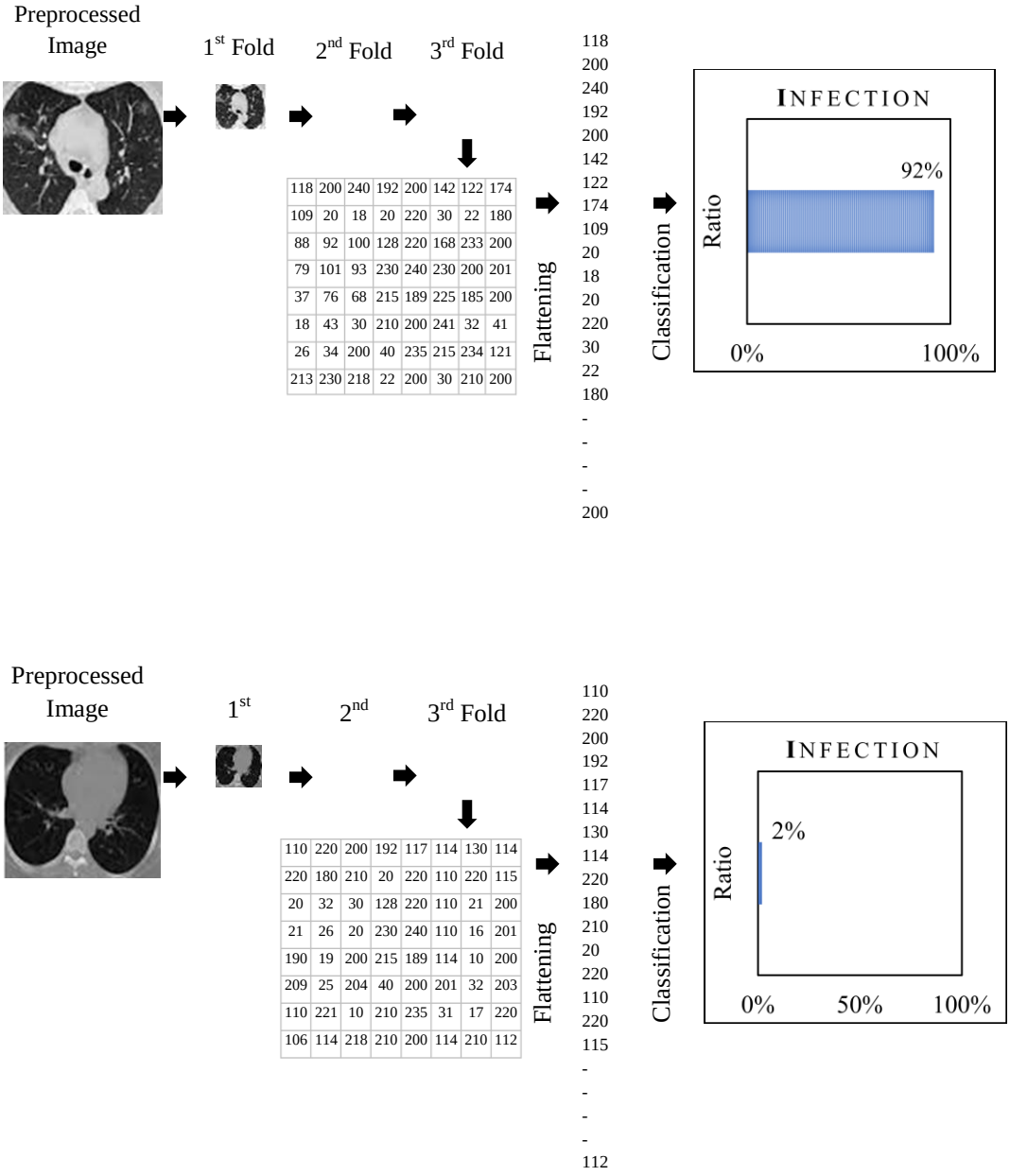

(B)

Figure 8. Two examples on classification stage, (A): for an infection case, (B): for a non-infection case.

6. Conclusion

The COVID-19 pandemic was a fundamental and influential event in the world, as it worked to change the features of the world by imposing new preventive habits, new treatment methods, and new detection methods since 2019. The alarm bell rang, and to this day, this epidemic was caused by a virus that affects the bronchi, lungs, and breathing, which is the cause of many deaths and is still in the process of transformation and development. From this point of view, many medical systems were proposed to detect the presence of the coronavirus in the lungs based on CT -scans. It was developed and simulated by applying a set of processing steps for the selected data. The classification method was performed based on deciding the presence or absence

of infection. Choosing a deep learning methodology gives an efficient tool for any related proposed system. We presented in this research an efficient system to distinguish automatically the presence or absence of coronavirus in CT-Scan images based on a developed CCN. The performance of our system has reached excellent results regarding its accuracy by applying it to our selected CT-Scan images. The proposed system was trained and tested accurately without any problem affecting its performance. The training phase was executed perfectly in reasonable training time and number of iterations with the clear presence of the cost function's gradient and its stable local optima without encountering overfitting. The developed system overcame many challenges and gaps in the related research and revealed results in the testing phase, making it capable of classifying unseen images it didn't train on. The standard well-known metric of artificial intelligence concluded an achievement that our system had reached a perfect classifier with an AUC of 0.95, which means a significant performance in the medical classification and notable capacity distinguishing the studied CT-scan images in both infection and non-infection cases. The employed dataset is prepared carefully in the literature to develop our peer research. We aim to involve more data in the test set to prove the success of our developed system. From this standpoint, we project future work to enrich our dataset to generalize our work. Our presented work as it is presented doesn't have any limitations. We believe there is a low possibility that our future work will require us to address limitations resulting from testing our system on new data and thus it requires training on or adapting to new data.

7. Data Availability

As mentioned in section 5.1. of this paper, the datasets used in this study are available online free of charge.

References

[1] Alsharabi, N., Shahwar, T., Ur Rehman, A. and Alharbi, Y. (2023). Implementing Magnetic Resonance Imaging Brain Disorder Classification via AlexNet–Quantum Learning, *Mathematics, MPDI*, 11(376), 1-20. https://www.doi.org/10.3390/math11020376

[2] Aslan, M. (2022). CoviDetNet: A New COVID-19 Diagnostic System Based on Deep Features of Chest X-ray, *International Journal of Imaging Systems and Technology, Wiley*, 32(5), 1447-1463. https://www.doi.org/10.1002/ima.22771

[3] Bi, Q., Goodman, K. E., Kaminsky, J., and Lessler, J. (2019). What is Machine Learning? A Primer for the Epidemiologist, *American Journal of Epidemiology*, 188(12), 2222-2239, https://www.doi.org/10.1093/aje/kwz189

[4] Herpest, G., Lederlin, M., Naudin, M., Ohana, M., Chaumoitre, K., Gregory, J., Vilgrain, V., Freitag, C. A., De Margerie-Mellonst, C., Flory, V., Ludwig, M., Mondot, L., Fitton, I., Jacquier, A. R. R., Ardilouze, P., Petit, I., Gervaise, A., Bayle, O., Crombe, A., Sokeng, M. M., Thomas, C., Henry, G., Bliah, V., Le Tat , T., Guillot,. M., Gendrin, P., Garetier, M., Bertolle, E., Montagne, C., Langlet, B., Kalaaji, A., Kayayan, H., Desmots, F., Dhaene, B., Saulnier, P., Guillevin, R., Bartoli, J., Beregi, J., and Tasu, J. P. (2021). Efficacy of Chest CT for COVID-19 Pneumonia Diagnosis in France, *Radiology*,298(2), 81-87. http://www.doi.10.1148/radiol.2020202568

[5] Goodfellow, I, Bengio, Y, and Courville, A. (2016). Deep Learning. *MIT Press*, p. 326.

[6] Ijaz, A., Raza, B., Kiran, I., Waheed, A., Raza, A., Shah, H., and Aftan, S. (2023). Modality Specific CBAM-VGGNet Model for the Classification of Breast Histopathology Images via Transfer Learning, *IEEE Access*, 11, 15750–15762. http://www.doi.10.1109/ACCESS.2023.3245023

[7] Islam, M. M., Karray, F., Alhajj, R., and Zeng, J. (2021). A Review on Deep Learning Techniques for the Diagnosis of Novel Coronavirus (COVID-19), *IEEE Access*, 9,30551–30572. http://www.doi.10.1109/ACCESS.2021.3058537

[8] Jiang, W., Synovic, N., Hyatt, M., Schorlemmer, T. R., Sethi, R., Lu, Y. H., Thiruvathukal, G. K., and Davis, J. C. (2023). An Empirical Study of Pre-Trained Model Reuse in the Hugging Face Deep Learning Model Registry. *Proceedings of the ACM/IEEE 45th International Conference on Software Engineering (ICSE)*, 1-14. http://www.doi.10.48550/arXiv.2303.02552

[9] Kovác, A., Palásti, P., Veréb, D., Bozsik, B., Palkó, A., and Kincses, Z. T., (2021), The Sensitivity and Specificity of Chest CT in the Diagnosis of COVID-19. *European Radiology*, 31(5), 2819–2824. http://www.doi.10.1007/s00330-020-07347-x

[10] Liu, H., and Lang, B. (2019). Machine Learning and Deep Learning Methods for Intrusion Detection Systems: A Survey. *Applied Sciences (Switzerland)*, 9(20). http://www.doi.10.3390/app9204396

[11] Mehboob, F., Rauf, A., Jiang, R., Saudagar, A. K. J., Malik, K. M., Khan, M. B., Hasnat, M. H. A., AlTameem, A., and AlKhathami, M. (2022). Towards Robust Diagnosis of COVID-19 using Vision Self-attention Transformer. *Scientific Reports*, 12(1),1–12. http://www.doi.10.1038/s41598-022-13039-x

[12] N. Sarang, (2018), "Understanding AUC - ROC Curve", Towards Data Science, https://towardsdatascience.com/understanding-auc-roc-curve-68b2303cc9c5

[13] Owida, A., Galal, N. M., Elrafie, A. (2022). Decision-making Framework for a Resilient Sustainable Production System During COVID-19: An Evidence-based Research, *Computers and Industrial Engineering, Elsevier* ,164, 1-14 http://www.doi.10.1016/j.cie.2021.107905.

[14] Piramuthu, S. (1999). Financial Credit-risk Evaluation with Neural and Neurofuzzy Systems. *European Journal of Operational Research*, 112(2), 310–321.

[15] Shah, F. M., Joy, S. K. S., Ahmed, F., Hossain, T., Humaira, M., Ami, A. S., Paul, S., Jim, M. A. R. K., and Ahmed, S. (2021). A Comprehensive Survey of COVID-19 Detection Using Medical Images. SN Computer Science, 2(6), 1–22. http://www.10.1007/s42979-021-00823-1

[16] Simonyan, K., Zisserman, A. (2015). Very Deep Convolutional Network (VDCNet) for Large-Scale Image Processing, *The International Conference on Learning Representations Computer Science, Computer Vision and Pattern Recognition, Cornell University*, 1-14. https://doi.org/10.48550/arXiv.1409.1556

[17] Soares, E., Angelov, P., Biaso, S., Higa Froes, M., and Kanda A., Daniel. (2020). SARS-COV-2 CT-Scan dataset: A large dataset of real patients CT scans for SARS-COV-2 identification, *medRxiv*, https://doi.org/10.1101/2020.04.24.20078584.

[18] Valueva, M.V.; Nagornov, N.N.; Lyakhov, P.A.; Valuev, G.V.; Chervyakov, N.I. (2020). "Application of the Residue Number System to Reduce Hardware Costs of the Convolutional Neural Network Implementation". *Mathematics and Computers in Simulation. Elsevier BV*, 177, 232–243. http://www.doi.10.1016/j.matcom

[19] Wu, D., Ying, Y., Zhou, M., Pan, J., & Cui, D. (2023). Improved ResNet-50 Deep Learning Algorithm for Identifying Chicken Gender. *Computers and Electronics in Agriculture, Elsevier Science Publishers B. V.*, 205(C), 1-10.

[20] Xu, B., Martín, D., Khishe, M., & Boostani, R. (2022). COVID-19 diagnosis using Chest CT Scans and Deep Convolutional Neural Networks Evolved by IP-based Sine-Cosine Algorithm, *Medical and Biological Engineering and Computing*, 60(10), 2931–2949. http://www.doi.10.1007/s11517-022-02637-6

[21] Yousif, W. K., & Ali, A. A. (2020). Simulation of Pose to Pose Moving of the Mobile Robot with Specified GPS Points, Journal of Engineering, 26(11), 195–208. http://www.doi.10.31026/j.eng.2020.11.13

[22] Zhang, J., Zhang, Y., Jin, Y., Xu, J., Xu, X. (2023). Mdu-net: Multi-scale Densely Connected U-net for Biomedical Image Segmentation, *Health Information Science and Systems*, 11(1), 1-13. http://www.doi.10.1007/s13755-022-00204-9